Journal of Solid State Chemistry **168,** 69–75 (2002)
doi:10.1006/jssc.2002.9681

Structural Study of an Unusual Cubic Pyrochlore $Bi_{1.5}Zn_{0.92}Nb_{1.5}O_{6.92}$

I. Levin,*[,1] T. G. Amos,* J. C. Nino,† T. A. Vanderah,* C. A. Randall,† and M. T. Lanagan†

**Materials Science and Engineering Laboratory, National Institute of Standards and Technology, Gaithersburg, Maryland 20899; and †Center for Dielectric Studies, Materials Research Laboratory, The Pennsylvania State University, University Park, Pennsylvania 16802*

Received February 5, 2002; in revised form May 28, 2002; accepted June 17, 2002

Single-phase pyrochlore-type specimens of $Bi_{1.5}Zn_{0.92}Nb_{1.5}O_{6.92}$ were studied using combined electron, X-ray and neutron powder diffraction techniques. Rietveld refinements using neutron powder diffraction data confirmed an average pyrochlore structure $A_2B_2O_6O'$ ($Fd\bar{3}m$, $a = 10.5616(1)$ Å) with both Bi and Zn mixed on the *A*-sites. However, refinements revealed significant local deviations from the ideal pyrochlore arrangement which were caused by apparent displacive disorder on both the *A* and O′ sites. The best fit was obtained with a disordered model in which the *A*-cations were randomly displaced by ∼0.39 Å from the ideal eight-fold coordinated positions. The displacements occur along the six ⟨112⟩ directions perpendicular to the O′–*A*–O′ links. In addition, the O′ ions were randomly displaced by ∼0.46 Å along all 12 ⟨110⟩ directions. Crystal–chemical considerations suggest the existence of short-range correlations between the O′ displacements and both the occupancy of the *A*-sites (i.e., Bi or Zn) and the directions of the *A*-cation displacements. The combined *A*-cation and O′ displacements change the coordination sphere of the *A*-cations from 8 to (5+3); the resulting coordination environment of the *A*-cations bears similarities to that of the (5+1)coordinated Zn in zirconolite-like $Bi_2Zn_{2/3}Nb_{4/3}O_7$. The observed displacive disorder in the A_2O' network of the $Bi_{1.5}Zn_{0.92}Nb_{1.5}O_{6.92}$ structure involves atoms associated with the lowest-frequency vibrational bending mode, and is likely responsible for both the high dielectric constant and the dielectric relaxation reported for this compound. © 2002 Elsevier Science (USA)

Key Words: **Pyrochlore; dielectric; Bismuth zinc niobate; disorder.**

INTRODUCTION

Ternary oxides in the Bi_2O_3–ZnO–Nb_2O_5 (BZN) system exhibit high dielectric constants (ε), relatively low dielectric losses, and compositionally tunable temperature coefficients of capacitance (τ_c) (1). Such properties, combined with sintering temperatures of less than 950°C, render these materials attractive candidates for capacitor and high-frequency filter applications in multilayer structures cofired with silver electrodes (2–4). The system reportedly features two structurally distinct ternary compounds, $Bi_{1.5}ZnNb_{1.5}O_7$ ($\varepsilon \approx 145$, $\tau_c \approx -400$ ppm/°C) and $Bi_2Zn_{2/3}Nb_{4/3}O_7$ ($\varepsilon \approx 80$, $\tau_c \approx +200$ ppm/°C), exhibiting very dissimilar dielectric properties (1–4). Since the two compounds exhibit opposite signs of τ_c, their mixture yields temperature-compensated ceramics (3, 4). $Bi_{1.5}ZnNb_{1.5}O_7$ ceramics exhibit low-temperature dielectric relaxation, attributed to a dipolar glass-like mechanism, while no such behavior was observed for $Bi_2Zn_{2/3}Nb_{4/3}O_7$ in the same temperature range (3, 4). Despite growing technological interest in these materials, understanding of their dielectric behavior has been impeded by the lack of detailed structural information. Based on the nominal composition and the indexed X-ray powder diffraction patterns, the $Bi_{1.5}ZnNb_{1.5}O_7$ compound was claimed to exhibit a cubic pyrochlore structure $A_2B_2O_7$, implying that the Zn ions occupy both *A*- and *B*-sites (5). However, in the absence of detailed structural/compositional data, the presence of rather small Zn ions (6) on the eight-fold coordinated *A*-sites remained controversial (7, 8), because the ionic radius of Zn falls outside the known limits of structural stability for pyrochlores (9). The other compound, $Bi_2Zn_{2/3}Nb_{4/3}O_7$, was reported to crystallize with a distorted pyrochlore structure (6); however, it was recently confirmed that this compound adopts a monoclinic zirconolite-like arrangement (space group $C2/c$, $a = 13.1037(9)$ Å, $b = 7.6735(3)$ Å, $c = 12.1584(6)$ Å, $\beta = 101.318(5)$) (10). The zirconolite structure, which, like pyrochlore, can be described as an anion-deficient fluorite derivative, features a distinct type of cation arrangement on the metal sites and cannot be derived from the pyrochlore structure by a distortion (11, 12). In the present report, we describe a detailed structural analysis of the cubic pyrochlore phase in the BZN system using X-ray and neutron

---

[1] To whom correspondence should be addressed. Bldg. 223/A256, NIST, Gaithersburg, MD 20899, U.S.A. Fax: 301-975-5334. E-mail: igor.levin@nist.gov.

0022-4596/02 $35.00

powder diffraction combined with transmission electron microscopy.

EXPERIMENTAL PROCEDURE

Specimens along the compositional line ZnO–$BiNbO_4$ were prepared by solid-state reaction of stoichiometric amounts of reagent grade Bi_2O_3, ZnO, and Nb_2O_5. The mixtures were ground for 24 h as aqueous slurries (60 vol% solids) using zirconia media. The resulting powders were subsequently dried at 120°C and calcined at 800°C for 4 h in closed alumina crucibles. Following calcination, the powders were re-milled for 24 h as aqueous slurries, dried at 120°C, and uniaxially pressed into pellets about 6 mm in diameter and 2 mm in thickness; 2 wt% organic binder was added to the powder to assist in forming. The pellets were sintered in flowing air (500 cm^3/min) at 950°C for 4 h. All samples were light yellow or ivory in color.

Specimens were initially characterized by X-ray powder diffraction using an automated Phillips θ–2θ Bragg–Brentano diffractometer equipped with Soller slits, a theta-compensating divergence slit, a graphite monochromator, and a scintillation detector. Data were collected using Cu$K\alpha$ radiation with a 0.015° step size and 8 s count time.

Specimens of composition $Bi_{1.5}ZnNb_{1.5}O_7$ were found to be mixtures of a cubic pyrochlore phase ($a = 10.552(1)$ Å, in agreement with other reports), and small amounts of ZnO (Fig. 1a). However, a single-phase (by X-ray powder diffraction) pyrochlore-type compound was obtained at the composition $Bi_{1.5}Zn_{0.92}Nb_{1.5}O_{6.92}$ (Fig. 1b). Detailed studies of phase equilibria in the Bi_2O_3–ZnO–Nb_2O_5 system are in progress to establish exact boundaries of the pyrochlore phase field. Synthesis of the $Bi_{1.5}Zn_{0.92}Nb_{1.5}O_{6.92}$ specimen was repeated in platinum capsules sealed by welding. Stoichiometric amounts of Bi_2O_3 (99.9%), ZnO (99.99%) and Nb_2O_5 (99.9985%) were mixed by grinding in acetone for 15 min with an agate mortar and pestle. The mixture was heated in a sealed Pt capsule at 800°C for 4 h, yielding a partially reacted product consisting of zirconolite-type Bi–Zn–Nb–O as the major phase, with minor amounts of a pyrochlore-type phase, ZnO, and $ZnNb_2O_6$. After this mixture was reground for 15 min, sealed in a Pt capsule, and heated at 950°C for 4 h, a single-phase pyrochlore-type specimen was obtained, with an X-ray powder diffraction pattern matching that of the same composition prepared by the first method. Leakage of the Pt capsule was checked by quenching in water—the contents remained dry. Visual inspection revealed the interior walls of the capsule to be shiny and non-corroded; X-ray diffraction of this surface indicated only Pt and a trace of the cubic pyrochlore phase. These experiments indicate that, under the presently used conditions, ZnO + Bi_2O_3 react quickly to form stable phases, with insignificant volatalization. To check for the formation of a superstructure, a fully reacted sample of $Bi_{1.5}Zn_{0.92}Nb_{1.5}O_{6.92}$ was heated in a sealed Pt capsule at 600°C for 158 h, followed by quenching in water. No change in symmetry of the pyrochlore phase was detectable by either X-ray powder or electron diffraction.

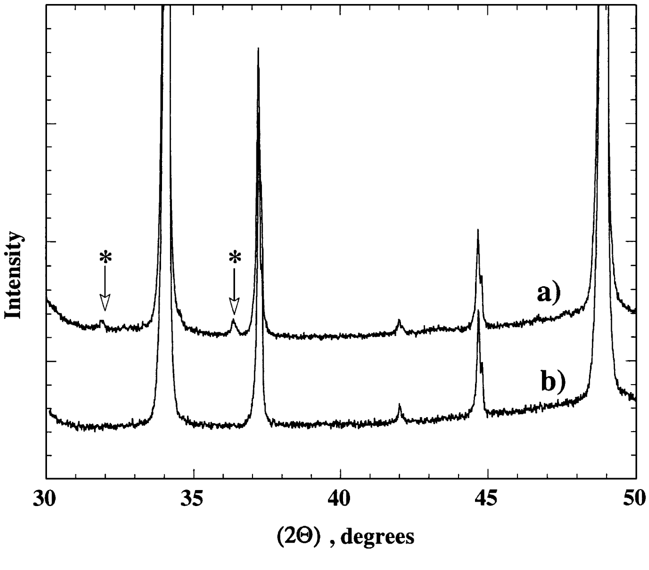

FIG. 1. X-ray powder diffraction patterns of (a) $Bi_{1.5}ZnNb_{1.5}O_7$ and (b) $Bi_{1.5}Zn_{0.92}Nb_{1.5}O_{6.92}$ specimens. The ZnO reflections in pattern (a) are indicated by asterisks; all other reflections are indexable according to the cubic unit cell with $a = 10.552(1)$ Å and $Fd\bar{3}m$ symmetry.

Polycrystalline $Bi_{1.5}Zn_{0.92}Nb_{1.5}O_{6.92}$ used for the detailed structural study was prepared by the first method. The composition of this specimen was analyzed using cold neutron prompt γ-ray activation analysis (PGAA) at the NIST Cold Neutron Research Facility (13). The technique involves sample irradiation by a beam of neutrons, resulting in neutron capture by different chemical elements. Upon de-excitation, nuclei emit prompt γ-rays with characteristic energies, which are registered using a high-resolution γ-ray detector. The element ratios are determined using the sensitivities of standard materials (14). The technique has high sensitivity to both Zn and Nb, but low sensitivity to Bi; therefore, only the Zn/Nb ratio was measured. A 2.5 g powder sample was sealed in a Teflon bag and placed in the CNPGAA chamber. The chamber was evacuated and the specimen was irradiated for 24 h. Prompt γ-rays were measured using a high-purity Ge detector. The absolute accuracy of the measurements was estimated using well-characterized $Bi_2Zn_{2/3}Nb_{4/3}O_7$ compound, for which the measurements produced Zn/Nb ratio of 0.51 ± 0.02 (2σ). PGAA analysis of the $Bi_{1.5}Zn_{0.92}Nb_{1.5}O_{6.92}$ specimen yielded Zn/Nb ratio of 0.59 ± 0.02 (2σ), which is in good agreement with the nominal value of 0.613. The composition $Bi_{1.5}Zn_{0.42}[Zn_{0.5}Nb_{1.5}]O_{6.92}$ suggests the unusual location of Zn on the relatively large A-sites.

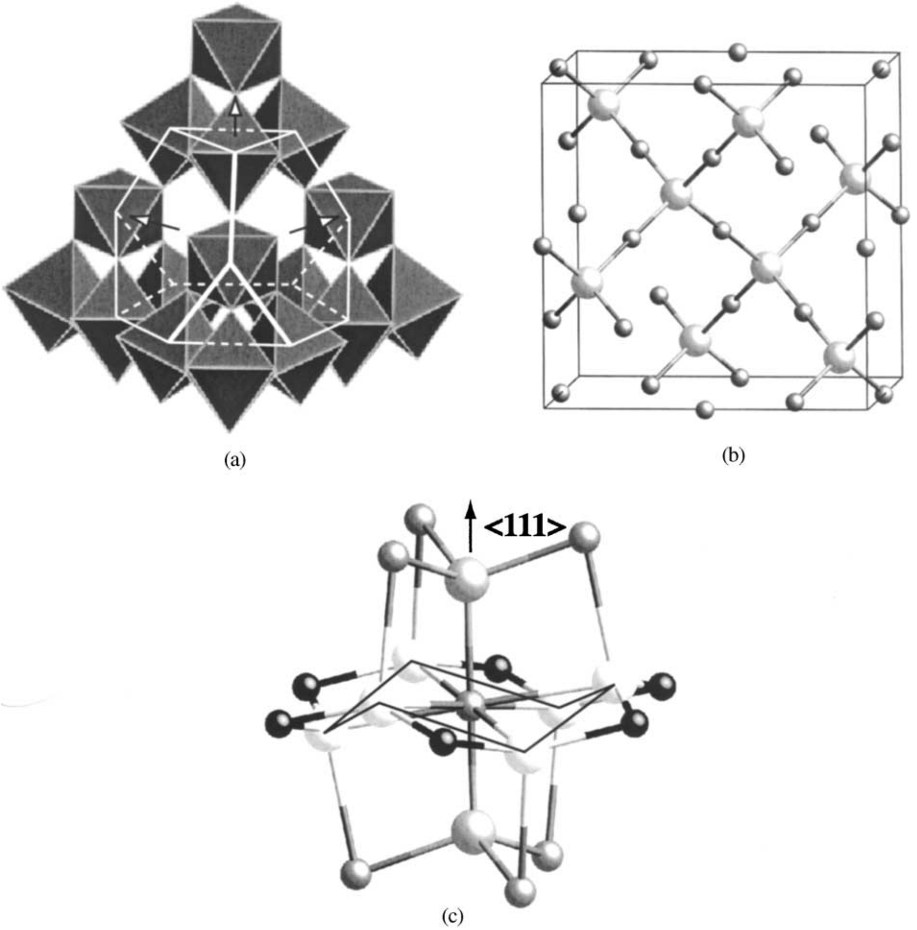

FIG. 2. Illustrations of the (a) B_2O_6 and (b) A_2O' interpenetrating networks in pyrochlore. Octahedra represent $[BO_6]$ units. Large spheres denote oxygen, smaller dark spheres are A-cations. $[BO_6]$ octahedra share all vertices to form the B_2O_6 three-dimensional framework based on the diamond net (a). The resulting large cavities contain the O′ and A atoms, themselves forming a second cuprite-like tetrahedral net (b). The B_2O_6 network consists of {111} sheets of octahedra-sharing corners to form three- and six-membered rings (outlined in (a)); the arrows indicate non-equivalent ⟨111⟩ directions. The two networks interpenetrate such that the A–O′–A linkages are perpendicular to the puckered six-membered rings of octahedra, resulting in eight-fold coordination of the A-cations, as shown in (c).

Specimens for transmission electron microscopy were prepared from sintered pellets by grinding and polishing followed by ion thinning until perforation was attained; the ion thinning was accomplished in a Gatan[2] precision ion-polishing system (PIPS) at 5 kV. The specimens were examined in conventional Phillips TEM 430 microscope operated at 200 kV.

Neutron powder diffraction data were collected at four different temperatures (298, 100, 50, and 12 K) at the NIST Center for Neutron Research reactor, NBSR. A Cu (311) monochromator with a 90 take-off angle, $\lambda = 1.5404(2)$ Å, and in-pile collimation of 15 min of arc were used. The sample (about 10 g) was loaded in vanadium can containers. Data were collected over the range 3–168 2θ with a step size of 0.05°. The GSAS package (15) was used for Rietveld structural refinement.

RESULTS AND DISCUSSION

The $A_2B_2O_7$ pyrochlore structure is often described by the formula $B_2O_6 \cdot A_2O'$, which emphasizes that the structure is built of two interpenetrating networks: $[BO_6]$ octahedra-sharing vertices form a three-dimensional network (Fig. 2a) based on a diamond net, and resulting in large cavities which contain the O′ and A atoms, themselves forming a second cuprite-like A_2O' tetrahedral net (Fig. 2b) (9). The octahedral B_2O_6 network consists of {111} sheets of octahedra, sharing corners to form six- and three-membered rings (Fig. 2a); these sheets are often referred to as "hexagonal tungsten bronze" (HTB) layers (12). The O′ ions, located between the HTB layers in the large cavities, are surrounded by four A cations with the $[A_4O']$

---

[2] The use of brand or trade names does not imply endorsement of the product by NIST.

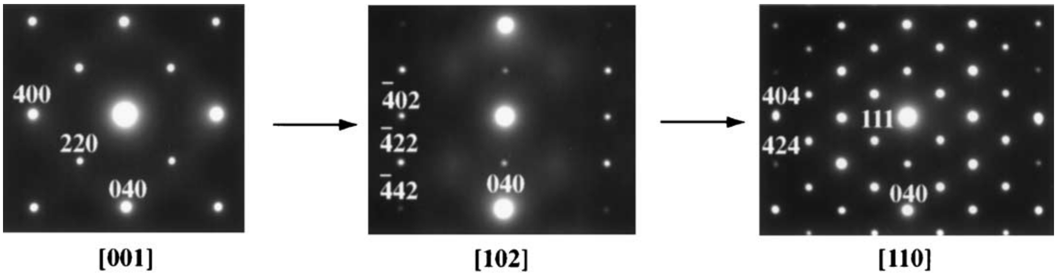

FIG. 3. Selected area electron diffraction patterns from the single grain in the $Bi_{1.5}Zn_{0.92}Nb_{1.5}O_{6.92}$ specimen. The reflections are indexed according to a cubic pyrochlore-type unit cell. The reflection conditions are consistent with the $Fd\bar{3}m$ space group. However, reflections 4 4 2 visible in both the ⟨110⟩ and ⟨112⟩ patterns violate special reflection conditions for the 8*b*, 16*c*, 16*d*, and 48*f* positions occupied in the ideal arrangement; these reflections were also visible in the X-ray and neutron powder diffaction patterns. (Note, that the 0 0 2 reflections in the ⟨110⟩ pattern, and $\bar{4}$02 reflections in the ⟨1 0 2⟩ pattern result from double diffraction as evident from their absence in the ⟨0 0 1⟩ orientation, where no routes for such double diffraction exist.)

tetrahedra-sharing corners. The *A*-cations are eight-fold coordinated by six O atoms in the octahedral framework, which form a puckered hexagonal ring in the HTB layer, and two O′ atoms, located so that the O′–*A*–O′ link is perpendicular to the puckered ring (Fig. 2c). The overall atomic arrangement results in a cubic unit cell with $a \approx 10$ Å and $Fd\bar{3}m$ symmetry; in the ideal arrangement the atoms occupy four special positions as the following: *A*-16*c*, *B*-16*d*, O-48*f* and O′-8*b* (9, 16).

Electron diffraction patterns from single grains of the $Bi_{1.5}Zn_{0.92}Nb_{1.5}O_{6.92}$ specimen were entirely consistent with both a pyrochlore-type unit cell and symmetry; the grains were free from extended defects (Fig. 3). However, several reflections (e.g., 442) observed in the experimental electron, X-ray, and neutron powder diffraction patterns, although accountable by the $Fd\bar{3}m$ symmetry, violate special reflection conditions for the 8*b*, 16*c*, 16*d*, and 48*f* sites (16) occupied in the ideal arrangement (Table 1); these observations suggest that some of the atoms are displaced to lower symmetry positions. Anomalies were also indicated by the results of Rietveld refinements using the ideal pyrochlore model (with vacancies on both the O′ and *A*-sites) which produced a rather poor fit ($R_{wp} = 6.39\%$, $R_{F2} = 7.43\%$, and $\chi^2 = 2.24$). The refinements generated abnormally large values of atomic temperature (displacement) parameters for both the O′ and (Bi/Zn) sites (Table 1). For the (Bi/Zn) *A*-cations, the principal components of the mean-square displacements directed perpendicular and parallel to the ⟨111⟩ directions are equal to $(U_{11}-U_{12}) \approx 0.14\,\text{Å}^2$ and $(U_{11}+2U_{12})) = 0.01\,\text{Å}^2$ (Table 1), respectively, suggesting that the *A*-cation displacements are confined to the {111} planes. The temperature parameters for the O atoms (48*f* sites) also were somewhat higher than normally accepted; these displacements appeared to be anisotropic, consistent with local tilting of $[(Nb,Zn)O_6]$ octahedra. The bond valence sum (BVS) (17) about the Nb/Zn *B*-site is equal to 4.14 v.u. $(0.75 \times 4.63 + 0.25 \times 2.65)$ which is close to the expected value of 4.25 v.u. However, the BVS = 2.03 v.u. $(0.75 \times 2.46_{Bi} + 0.21 \times 0.86_{Zn})$, calculated for the mixed Bi/Zn *A*-sites using refined bond distances ($|A\text{–}O'| = 2.29$ Å, $|A\text{–}O| = 2.67$ Å), is significantly smaller compared to the ideal value of 2.67 v.u. (0.75 × 3 v.u. + 0.21 × 2 v.u.). Thus, appreciable distortion of the *A*-site environment is expected to satisfy the bonding requirements of the *A*-cations. Abnormally large displacement parameters, along with relaxation of the special reflections conditions, suggest that this distortion is realized through (i) displacements of both *A*-cations and O′ anions from their ideal high symmetry positions (16*d*-*A*, 8*b*-O′), and (ii) local tilting of $[BO_6]$ octahedra.

The quality of the fit was improved significantly ($R_{wp} = 5.22\%$, $R_{F2} = 3.56\%$, $\chi^2 = 1.49$) by introducing displacive disorder on both *A* and O′ sites (Tables 2 and 3, Fig. 4). A combination of the best fit and most reasonable values of displacement parameters were obtained by placing both *A* and O′ ions on the 96*g* (*x*, *x*, *z*) positions. Similar positional parameters were obtained at both 298 and 12 K (Table 3), suggesting that the displacements are static in nature. The average residual bond strain around the *A*-cations was appreciably reduced in the disordered model: BVS = $(0.75 \times 2.86_{Bi} + 0.21 \times 1.00_{Zn})$ = 2.36 v.u.,[3] which is in fair agreement with the value of 2.67 v.u., calculated from site occupancies and formal charges, especially considering the existence of a lone pair on Bi^{3+} and vacancies in the structure; a further decrease in the bond strain is expected due to local tilting of $[BO_6]$ octahedra.

For the (Bi/Zn) cations, the refined displacement vector, **u** (expressed using fractional coordinates), is [0.033, 0.015, 0.015], which corresponds to a displacement of 0.037*a* (0.39 Å) approximately along the ⟨112⟩ direction. (Note that the square of this displacement, 0.15 Å^2, is close to the

---

[3] The experimental bond valence sum about the *A*-sites (Bi or Zn) was calculated from the valences of all the *A*–O′ and *A*–O bonds, generated by the disordered displacements of both (Bi/Zn) and O′ ions; the *A*–O′ and *A*–O bond abundances were normalized to 2 and 6, respectively.

TABLE 1
Atomic Positions and Isotropic Temperature Parameters Refined for the Ideal Pyrochlore ($Bi_{1.5}Zn_{0.92}Nb_{1.5}O_{6.92}$) Model Using Neutron Diffraction Data ($T = 298$ K)

Atom	Site	x	y	z	Occupancy	U_{iso}, Å$^2 \times 100$
O′	8*b*	$\frac{3}{8}$	$\frac{3}{8}$	$\frac{3}{8}$	0.92	11.28(21)
O	48*f*	0.3196(1)	$\frac{1}{8}$	$\frac{1}{8}$	1	2.34[a]
Bi/Zn	16*d*	$\frac{1}{2}$	$\frac{1}{2}$	$\frac{1}{2}$	0.75/0.21	9.87(11)[b]
Nb/Zn	16*c*	0	0	0	0.75/0.25	1.79(3)

[a] $U_{11} = 0.0352(5)$ Å^2, $U_{22} = U_{33} = 0.01746(26)$ Å^2, $U_{12} = U_{13} = 0$, $U_{23} = 0.0108(32)$ Å^2.

[b] $U_{11} = U_{22} = U_{33} = 0.0986(9)$ Å^2, $U_{12} = U_{23} = U_{13} = -0.0443(6)$ Å^2.

Note. Space group $Fd\bar{3}m$, $a = 10.56156(7)$ Å, $R_{wp} = 6.39\%$, $R_p = 5.25\%$, $R_{F2} = 7.43\%$, and $\chi^2 = 2.239$. The temperature parameters for both the O′ and Bi/Zn sites are abnormally large, suggesting displacements of these ions from the ideal 16*d* and 8*b* special positions.

TABLE 2
Experimental Parameters for Neutron Diffraction Studies of $Bi_{1.5}Zn_{0.92}Nb_{1.5}O_{6.92}$

	$T = 298$ K	$T = 12$ K
Unit cell (Space group $Fd\bar{3}m$, 227)	$a = 10.56156(7)$ Å Volume = 1178.11(1) Å^3	$a = 10.55668(6)$ Å Volume = 1176.47(1) Å^3
R_p (profile)	0.0519	0.0517
R_{wp} (weighted profile)	0.0427	0.0421
R_F^2 (Bragg)	0.0347	0.0310
Reduced χ^2	1.487	1.597
Total refined variables	38	
Minimum 2θ	3	
Maximum 2θ	165	
Number of reflections	85	
Profile function	Pseudo-Voight (GSAS type 3)	
Gaussian U, V, W	206, −243, 149	206, −244, 151
Cauchy X, Y	1.22, 0.0	0.99, 0.0
Background function	Chebyschev polynomial (18 coefficients)	

Note. The agreement factors are given for the refinements of the disordered model (Table 3).

mean-square displacement perpendicular to the ⟨111⟩ direction, 0.14 Å^2, which was refined for the ideal pyrochlore model.) In the disordered model, each A cation is randomly distributed over six sites, which are displaced from the ideal 16*c* positions approximately along the three ⟨112⟩ directions perpendicular to the corresponding O′–A–O′ link (Fig. 5a). The displacements of the A-cations are confined to the HTB layers, and result in shortening three out of six A–O bonds. The displacements of O′ ions occur along all six ⟨110⟩ directions (Fig. 5b), so that each of the O′ ion is distributed over 12 sites; the approximate magnitude of these displacements is 0.044a (0.46 Å).

The largest BVS about the A-sites (1.64 v.u. for Zn and 4.71 v.u. for Bi) is achieved when both O′ ions in the O′–A–O′ link move toward the corresponding HTB layer; these A-sites are expected to be occupied by Zn. Three other O′–A bonds for the same O′ ion will be stretched, so that those A-sites are likely to be occupied by Bi. Thus, coupling between the displacements of the O′ atoms, the

TABLE 3
Atomic Positions and Temperature Parameters Refined for the Pyrochlore ($Bi_{1.5}Zn_{0.92}Nb_{1.5}O_{6.92}$) Model with Disorder on the O′ and A = (Bi/Zn) Sites

Atom	Site	x	y	z	Occupancy	U_{iso}, Å$^2 \times 100$
O′	96*g*	0.34403(27)	0.34403(27)	0.3776(5)	0.0767	2.05(21)
		0.34361(23)	0.34361(23)	0.3761(4)		1.19(18)
O	48*f*	0.31984(7)	$\frac{1}{8}$	$\frac{1}{8}$	1.000	2.28a
		0.31965(6)	$\frac{1}{8}$	1.8		1.79b
Bi/Zn	96*g*	0.46731(34)	0.51499(35)	0.51499(35)	0.125/0.035	1.62(5)
		0.46800(31)	0.51671(31)	0.51671(31)		1.20(5)
Nb/Zn	16*c*	0	0	0	0.75/0.25	1.37(2)
		0	0	0		1.02(2)

[a] $U_{11} = 0.0330(5)$ Å^2, $U_{22} = U_{33} = 0.0177(2)$ Å^2, $U_{12} = U_{13} = 0$, $U_{23} = 0.0085(3)$ Å^2.

[b] $U_{11} = 0.0276(4)$ Å^2, $U_{22} = U_{33} = 0.0131(2)$ Å^2, $U_{12} = U_{13} = 0$, $U_{23} = 0.0066(3)$ Å^2.

Note. The upper and lower entries correspond to the temperatures 298 and 12 K, respectively. Lattice parameters for the 298 and 12 K are 10.56156(7) and 10.55668(6) Å, respectively. The space group is $Fd\bar{3}m$ (227, origin at 16*c*).

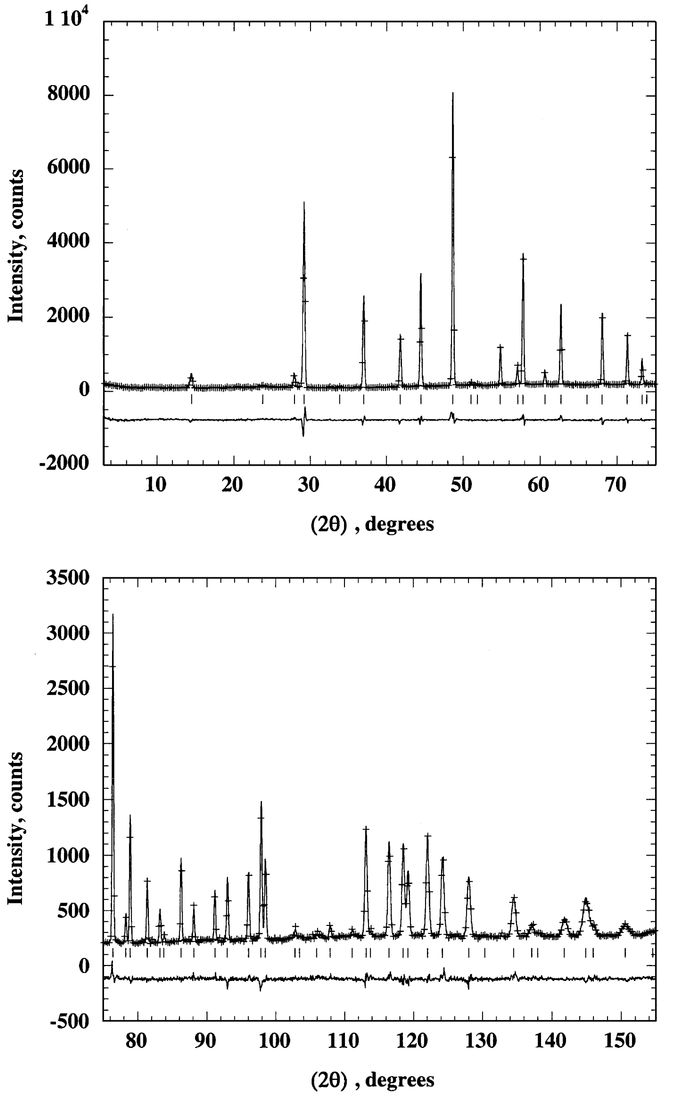

FIG. 4. (Upper) Experimental (crosses) and calculated (line) neutron powder diffraction profiles for $Bi_{1.5}Zn_{0.92}Nb_{1.5}O_{6.92}$ at 298 K. The calculated profile corresponds to the model described in Table 3. (Lower) Residual.

occupancy of the *A*-sites (Bi, Zn, or vacancy), and the directions of the *A*-cation displacements is expected. Because no superstructure reflections were observed, any such structural correlation must be short range in nature. Crystal–chemical considerations suggest local ordering in which each O′ ion is bonded to three Bi and one Zn cations: in such configurations bonding requirements of both Zn and Bi can be met. However, no characteristic streaks of diffuse intensity which could confirm the existence of tetrahedral [Bi_3ZnO'] clusters were observed in the electron diffraction patterns; apparently, analysis of a pair-distribution function using diffuse scattering in the X-ray/neutron powder diffraction data is necessary to establish local correlations in the structure of this compound.

The local environment of $A = (Bi/Zn)$ cations in the presently refined cubic pyrochlore-type $Bi_{1.5}Zn_{0.92}Nb_{1.5}O_{6.92}$ structure bears similarities to that of the (5 + 1)-coordinated Zn in zirconolite-like $Bi_2Zn_{2/3}Nb_{4/3}O_7$ (10, 11). Both structures contain hexagonal tungsten bronze (HTB) layers formed by vertex-linked [BO_6] octahedra. The interstices formed by the six-membered rings of octahedra in these layers are occupied by the *A*-cations in pyrochlore, and smaller transition metal cations in zirconolite (e.g., Ti in $CaZrTi_2O_7$ (11), and Zn in $Bi_2Zn_{2/3}Nb_{4/3}O_7$ (10)). In the ideal pyrochlore structure, the *A*-cations reside in the ring centers and are eight-fold coordinated by oxygen. In zirconolite, the transition metal cations are displaced away from the ring centers and statistically occupy two sites on both sides of the two-fold symmetry axes; the resulting coordination of these cations is (5 + 1).[4] The displacement vectors (from the ring centers) of Zn cations in $Bi_2Zn_{2/3}Nb_{4/3}O_7$ are approximately parallel to the $\langle 112 \rangle$ pseudo-cubic directions in the HTB layers (10), which is similar to the presently refined *A*-cation displacements in the pyrochlore structure. However, in the BZN pyrochlore, all 8 oxygen atoms surrounding the *A*-cation remain closer to it than the next-nearest-neighboring cations, and the resulting *A*-cation coordination is (5 + 3).

Recent studies of the BZN pyrochlore using far-infrared spectroscopy (18) indicated that the observed number of polar modes is larger than the seven expected for the ideal pyrochlore arrangement; these observations are consistent with displacements of some of the atoms to lower symmetry positions. The lowest-frequency polar infrared modes in pyrochlores are commonly assigned (in the order of increasing frequency) to the O′–*A*–O′ bending and O–*A*–O bending, respectively (9). According to the analysis of IR data for the cubic BZN pyrochlore (18), the lowest frequency O′–*A*–O′ bending mode provides the strongest contribution to the dielectric constant while the contribution of the O–*A*–O bending is also significant. Both types of bending resemble those produced by the presently identified static displacements of the *A*, O′ and O atoms; therefore, these displacements are expected to have a strong effect on the dielectric response of the cubic BZN pyrochlore-type compound. In particular, the apparent displacive disorder in the A_2O' network is the likely cause for the "glass-like" dielectric behavior of the pyrochlore phase.

CONCLUSIONS

Samples of composition $Bi_{1.5}ZnNb_{1.5}O_7$ consist of a cubic pyrochlore-type phase and small amounts of ZnO.

---

[4] The first coordination sphere of the cation was defined to include only those oxygen nearest neighbors which are closer to this cation than the next-nearest-neighboring cations.

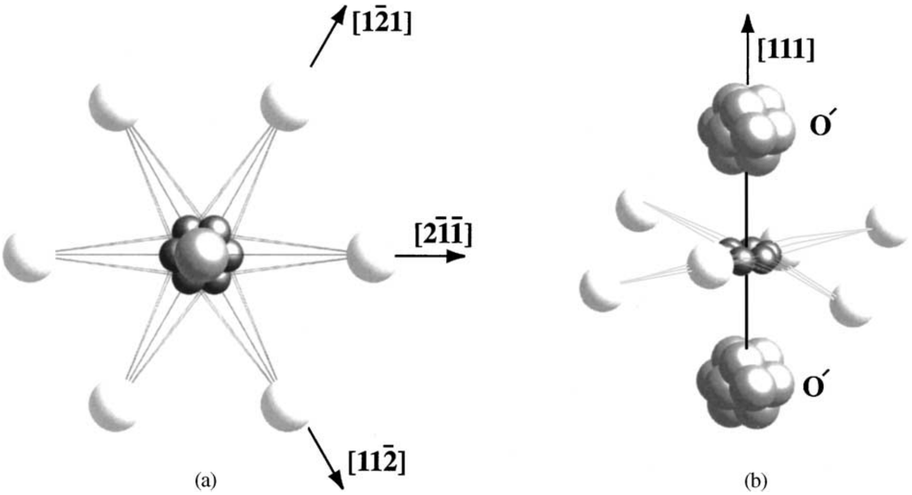

FIG. 5. Nearest-neighbor environment for the *A*-cations in the pyrochlore-type $Bi_{1.5}Zn_{0.92}Nb_{1.5}O_{6.92}$ indicated by the refinement results (Table 3). Large white and gray spheres represent O and O′ atoms, respectively, while smaller dark spheres correspond to the *A*-cations. (a) View along [111] direction with six randomly occupied *A*-cation positions indicated by dark spheres. The O′ atoms is shown at the ideal position for clarity. (b) View along the direction nearly perpendicular to the [111]. The displaced positions of both the *A* and O′ atoms are indicated.

However, the pyrochlore forms as a single phase at the composition $Bi_{1.5}Zn_{0.92}Nb_{1.5}O_{6.92}$. Electron, X-ray, and neutron powder diffraction patterns for this composition are consistent with both the cubic pyrochlore unit cell and $Fd\bar{3}m$ symmetry. Rietveld refinements using neutron powder diffraction data confirmed an overall $B_2O_6 \cdot A_2O'$ cubic pyrochlore structure with Zn cations present on both *A*- and *B*-sites; i.e., $Bi_{1.5}Zn_{0.92}[Zn_{0.5}Nb_{1.5}]O_{6.92}$. However, the refinement results indicated significant local deviations from the ideal pyrochlore arrangement, and suggested substantial displacive disorder in the A_2O' network. In particular, the (Bi/Zn) *A*-cations were found to be displaced along one the six $\langle 112 \rangle$ directions parallel to the corresponding HTB layers. In contrast, the O′ ions are displaced along all 12 $\langle 110 \rangle$ directions; correlations between the directions of O′ displacements, the occupancy of the *A*-sites, and the directions of the *A*-cation displacements are expected, but could not be ascertained from the present data. The combined *A*-cation and O′ displacements reduce residual tensile bond strain around the *A*-cations. The resulting oxygen environment of the *A*-cations in the $Bi_{1.5}Zn_{0.92}Nb_{1.5}O_{6.92}$ cubic pyrochlore bears similarities to that of the (5+1)-coordinated Zn cations in zirconolite-type $Bi_2Zn_{2/3}Nb_{4/3}O_7$. The identified atomic displacements involve atoms participating in the lowest-frequency O′–*A*–O′ bending mode, and therefore are likely responsible for both the high dielectric constant and low-temperature dielectric relaxation exhibited by this phase.

ACKNOWLEDGMENTS

The authors thank A. Santoro and R. S. Roth for useful discussions.

REFERENCES

1. D. P. Cann, C. A. Randall, and T. R. Shrout, *Solid State Commun.* **100**(7), 529–534 (1996).
2. M. Valant and P. K. Davies, *J. Am. Ceram. Soc.* **83**(1), 147–153 (2000).
3. J. C. Nino, M. T. Lanagan, and C. A. Randall, *J. Appl. Phys.* **89**(8), 4512–4516 (2001).
4. J. C. Nino, M. T. Lanagan, and C. A. Randall, *J. Mater. Res.* **16**(5), 1460–1464 (2001).
5. X. Wang, H. Wang, and X. Yao, *J. Am. Ceram. Soc.* **80**(10), 2745–2748 (1997).
6. R. D. Shannon, *Acta Crystallogr. A* **32,** 751 (1976).
7. A. Mergen and W. E. Lee, *Mater. Res. Bull.* **32,** 175 (1997).
8. G. Jeanne, G. Desgardin, and B. Raveau, *Mater. Res. Bull.* **9,** 1321–1332 (1974).
9. M. A. Subramanian, G. Aravamudan, and G. V. Subba Rao, *Prog. Solid State Chem.* **15**(2), 55–143 (1983).
10. I. Levin, T. G. Amos, J. C. Nino, T. A. Vanderah, I. M. Reaney, C. A. Randall, and M. T. Lanagan, *J. Mater Res.* **17**(6), 1406–1411 (2002).
11. B. M. Gatehouse, I. E. Grey, R. J. Hill, and H. J. Rossel, *Acta Crystallogr. B* **37,** 306–312 (1981).
12. T. J. White, *Am. Miner.* **69,** 1156–1172 (1984).
13. R. M. Lindstrom, *J. Res. Natl. Inst. Stand. Technol.* **98,** 127 (1993).
14. R. L. Paul, *J. Radioanal. Nucl. Chem. Ar* **191**(2), 245 (1995); 55–143 (1983).
15. A. C. Larson and R. B. Von Dreele, "General Structure Analysis System," Los Alamos National Laboratory Report LAUR 86-748, 1994.
16. T. Hahn (Ed.), "International Tables of Crystallography," Vol. A, Kluwer Academic Publishers, Dordrecht, 1996.
17. I. D. Brown and D. Altermatt, *Acta Crystallogr. B* **41,** 244–247 (1985).
18. S. Kamba, 2002, to be published.